Synthesis of *cis*- and *trans*-Dibenzo-30-Crown-10 Derivatives *via* Regioselective Routes and Their Complexations with Paraquat and Diquat

Chunlin He, Zuming Shi, Qizhong Zhou, Shijun Li, Ning Li,

and Feihe Huang*

Department of Chemistry, Zhejiang University, Hangzhou 310027, P. R. China. Fax: 86 571 8795 1895; Tel: 86 571 8795 3189; Email address: fhuang@zju.edu.cn

Supporting Information (33 pages)

1. Determination of association constants of *1•3*, *2•3*, *1•4*, and *2•4*[S1]

$K_{a,\mathbf{1•3}}$, $K_{a,\mathbf{2•3}}$, $K_{a,\mathbf{1•4}}$, and $K_{a,\mathbf{2•4}}$ were determined in the same way based on UV-Vis data. *cis*-Dibenzo-30-crown-10 diol **1** (or *trans*-dibenzo-30-crown-10 diol **2**) (5.00 × 10^{-3} mmol, 2.98 mg) were carefully added to a 10 mL volumetric flask. Then acetone was added to give a 0.500 mM solution of **1** (**2**). Precisely weighed guests (**3**, **4**) were dissolved in this 0.500 mM solution of **1** (or **2**) to afford 20.0 mM guest solutions. Titration of a guest solution into a specified volume of a host solution results in an increase of the absorbance intensity of the charge-transfer band of the complexes. Treatment of the collected absorbance data at $\lambda = 403$ nm with a non-linear curve-fitting program afforded the corresponding association constants.

The non-linear curve-fitting was based on the equation:

$$A = (A_\infty/[\text{H}]_0)\,(0.5[\text{G}]_0 + 0.5([\text{H}]_0+1/K_a)-(0.5\,([\text{G}]_0{}^2+(2[\text{G}]_0(1/K_a - [\text{H}]_0)) + (1/K_a + [\text{H}]_0)^2)^{0.5})) \qquad \text{(Eq. S1)}$$

Where A is the absorption intensity of the charge-transfer band ($\lambda = 403$ nm) at $[\text{G}]_0$, A_∞ is the absorbance intensity of the charge-transfer band ($\lambda = 403$ nm) when the host is completely complexed, $[\text{H}]_0$ is the fixed initial concentration of the host, and $[\text{G}]_0$ is the initial concentration of the guest.

a

b

R² = 0.99954

$A_{infinite}$ 0.18514 ±0.00153

K_a $1.1*10^3$ ±24
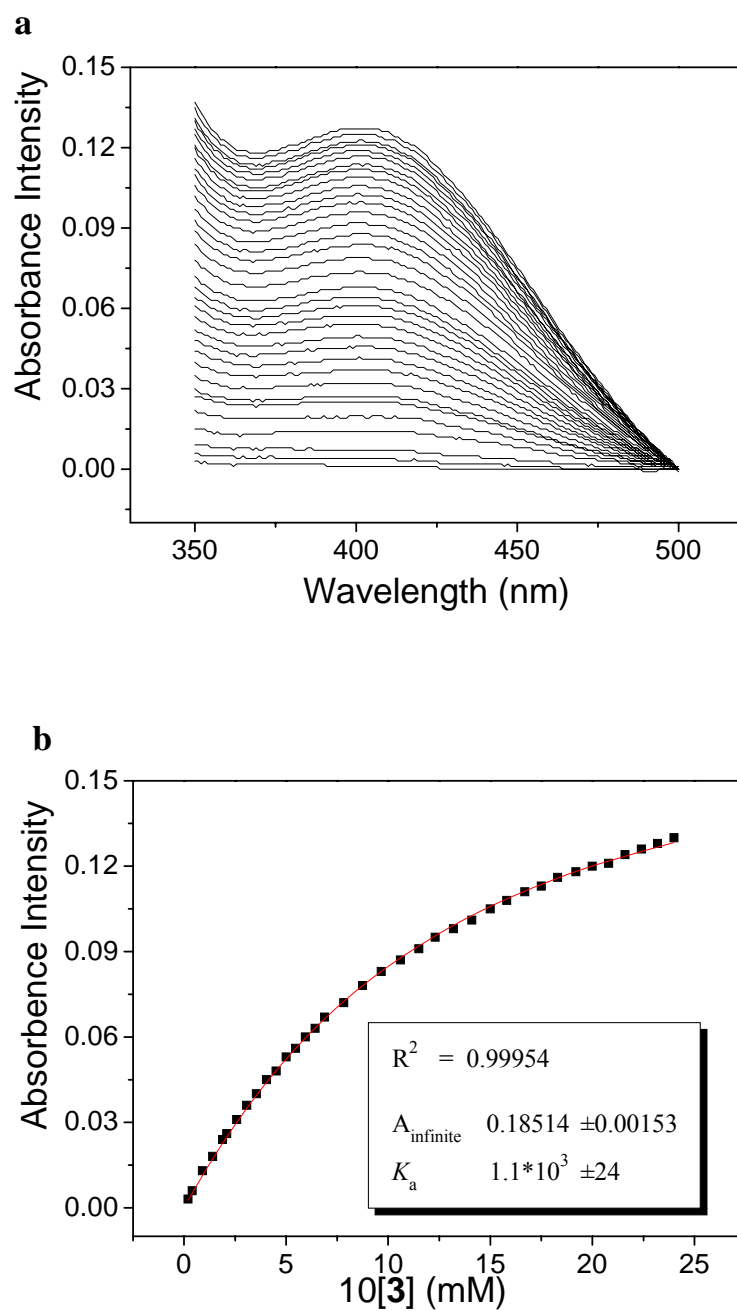
FIGURE S1. (a) The absorption spectral changes of **1** (0.500 mM) upon addition of **3** and (b) the absorbance intensity changes at λ = 403 nm upon addition of **3** (from 0 to 2.28 mM). The red solid line was obtained from the non-linear curve-fitting using Eq. S1.

c

d

R^2 = 0.99932

A$_{infinite}$ 0.14104 ±0.00187
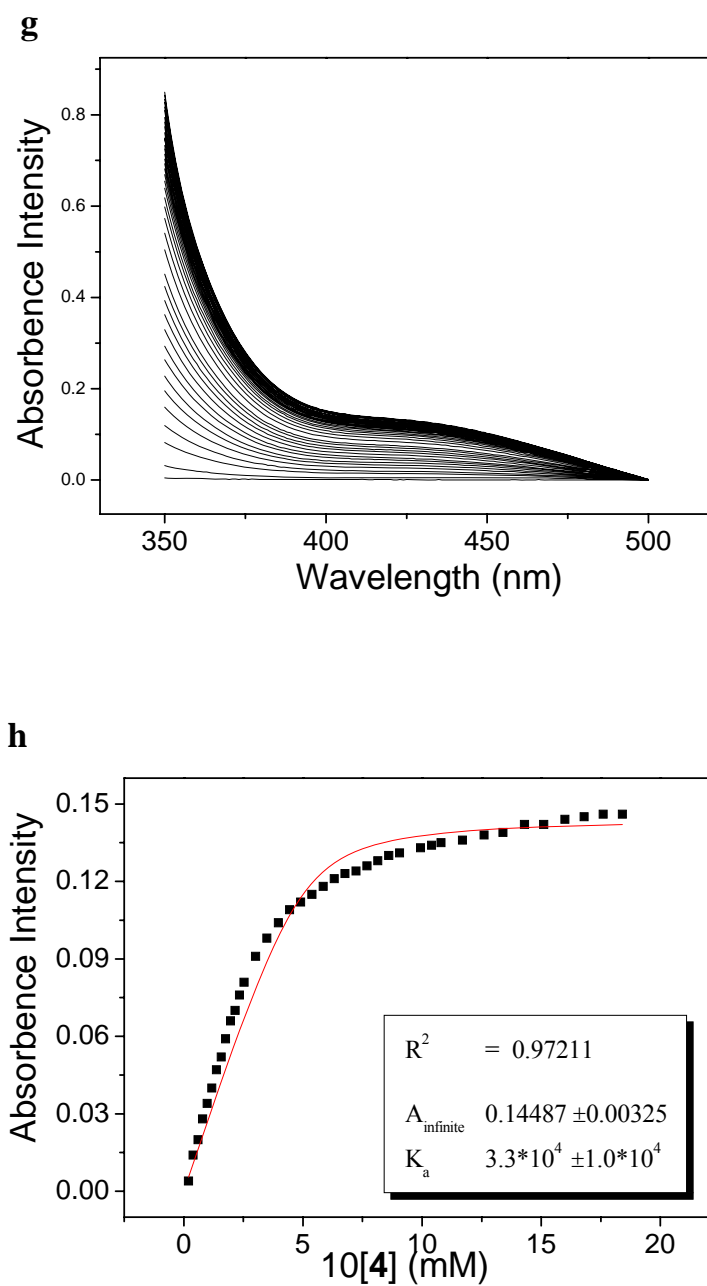
K$_a$ 1.7*10^3 ±56
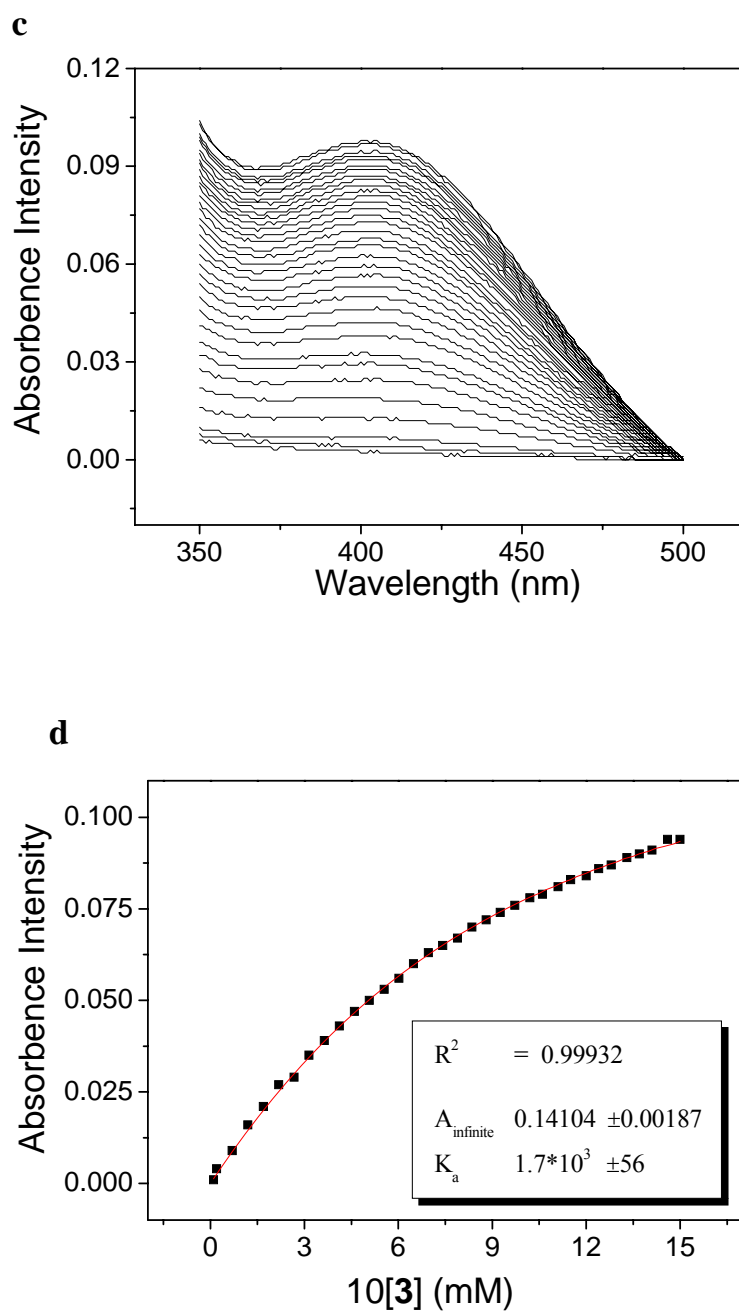
FIGURE S2. (c) The absorption spectral changes of **2** (0.500 mM) upon addition of **3** and (d) the absorbance intensity changes at $\lambda = 403$ nm upon addition of **3** (from 0 to 2.35 mM). The red solid line was obtained from the non-linear curve-fitting using Eq. S1.

e

f

$$R^2 = 0.98939$$

$$A_{infinite} \quad 0.15432 \pm 0.00167$$

$$K_a \quad 5.0*10^4 \pm 1.3*10^4$$
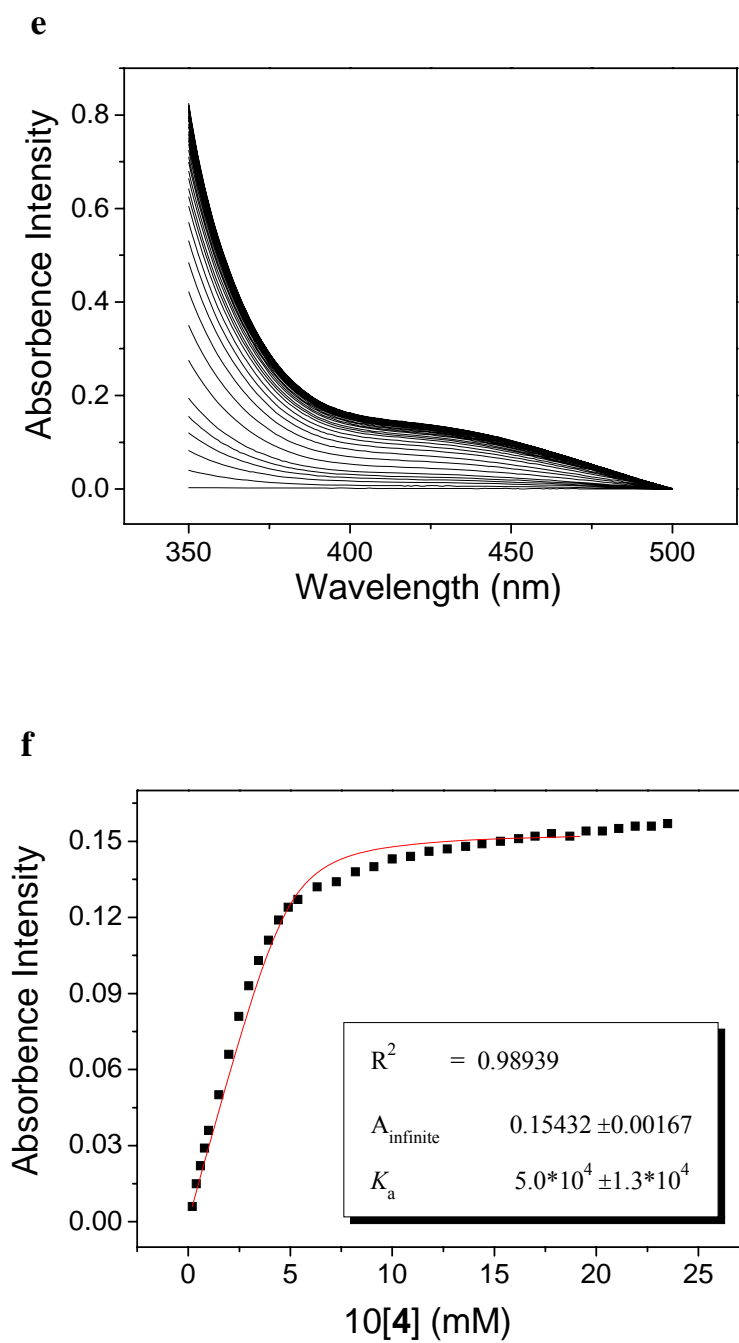
FIGURE S3. (e) The absorption spectral changes of **1** (0.500 mM) upon addition of **4** and (f) the absorbance intensity changes at $\lambda = 403$ nm upon addition of **4** (from 0 to 1.63 mM). The red solid line was obtained from the non-linear curve-fitting using Eq. S1.

g

h

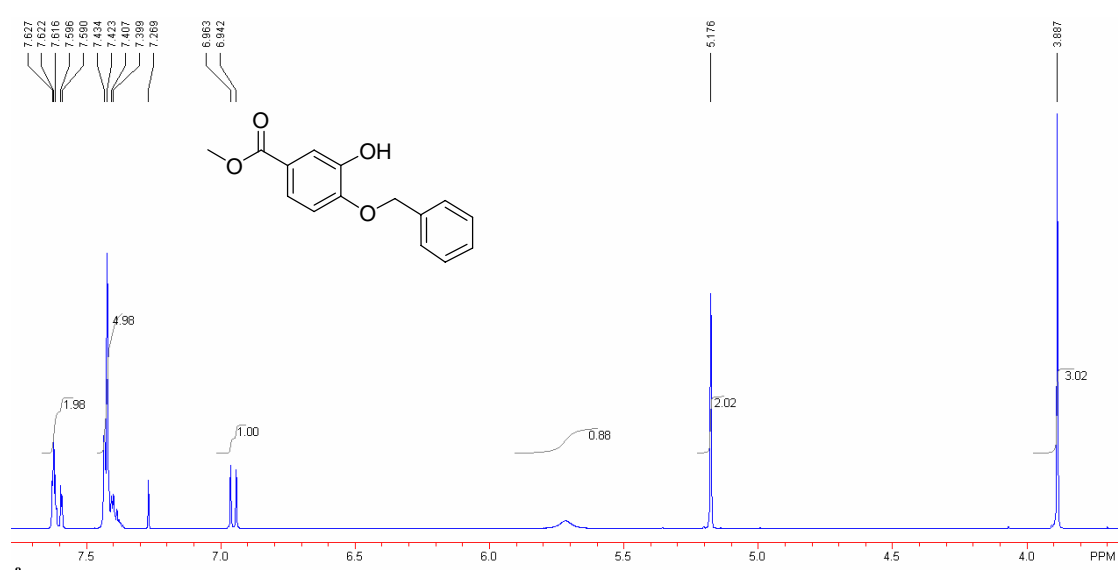|	
R^2	$= 0.97211$
$A_{infinite}$	0.14487 ± 0.00325
K_a	$3.3*10^4 \pm 1.0*10^4$

FIGURE S4. (g) The absorption spectral changes of **2** (0.500 mM) upon addition of **3** and (h) the absorbance intensity changes at $\lambda = 403$ nm upon addition of **3** (from 0 to 1.82 mM). The red solid line was obtained from the non-linear curve-fitting using Eq. S1.
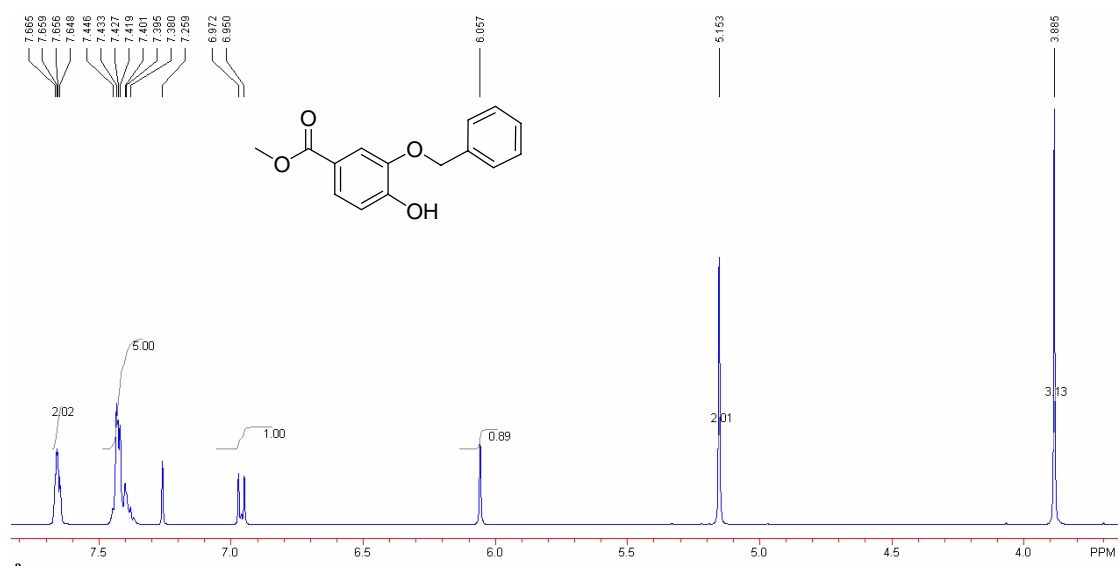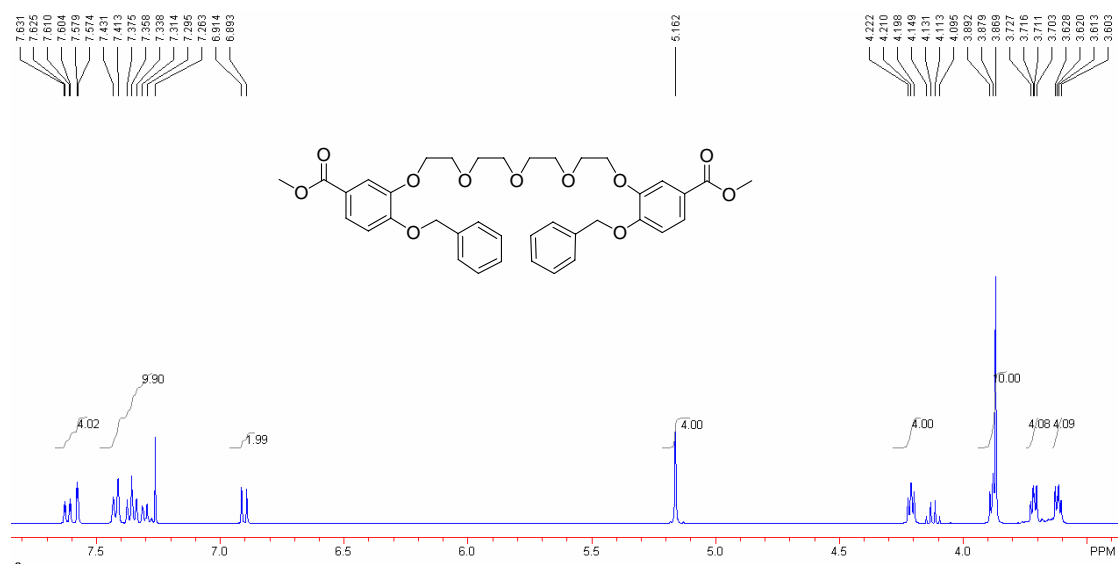
2. ^{1}H NMR spectra of compounds
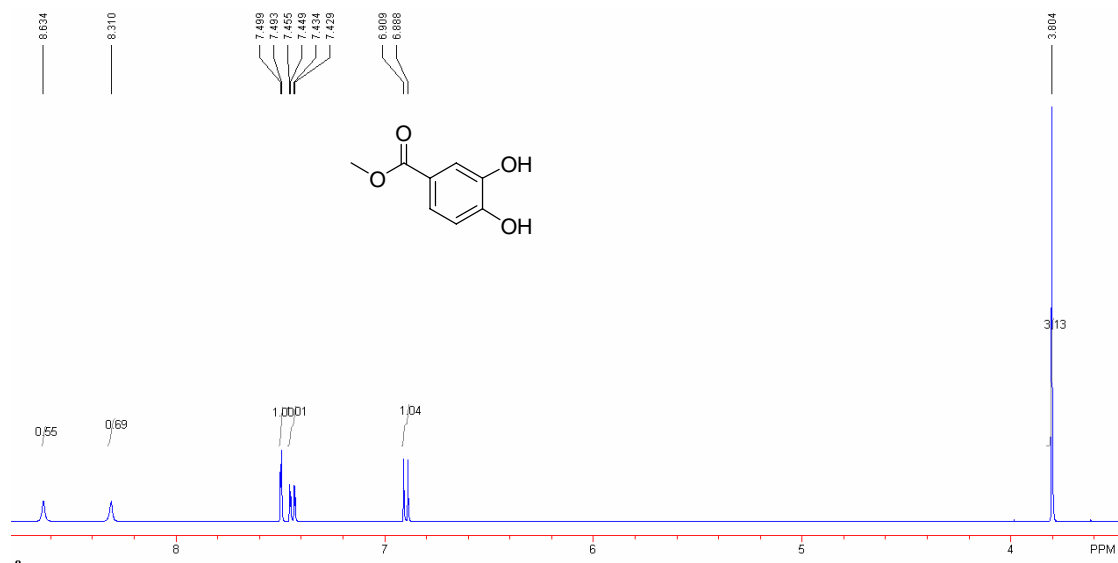
FIGURE S5. ^{1}H NMR spectrum (400 MHz, CD$_3$COCD$_3$, 22 °C) of **6**.

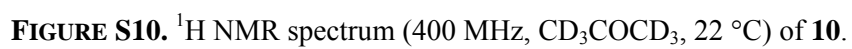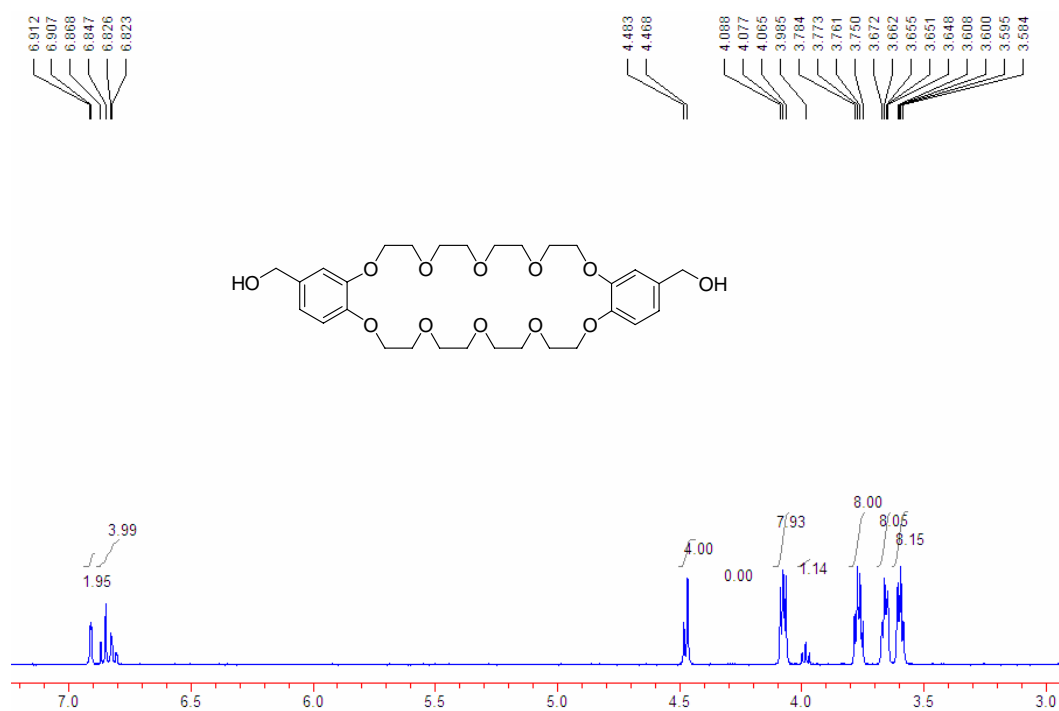**FIGURE S6.** ^{1}H NMR spectrum (400 MHz, CDCl$_3$, 22 °C) of **7a**.

FIGURE S7. ^{1}H NMR spectrum (400 MHz, CDCl$_3$, 22 °C) of **7b**.

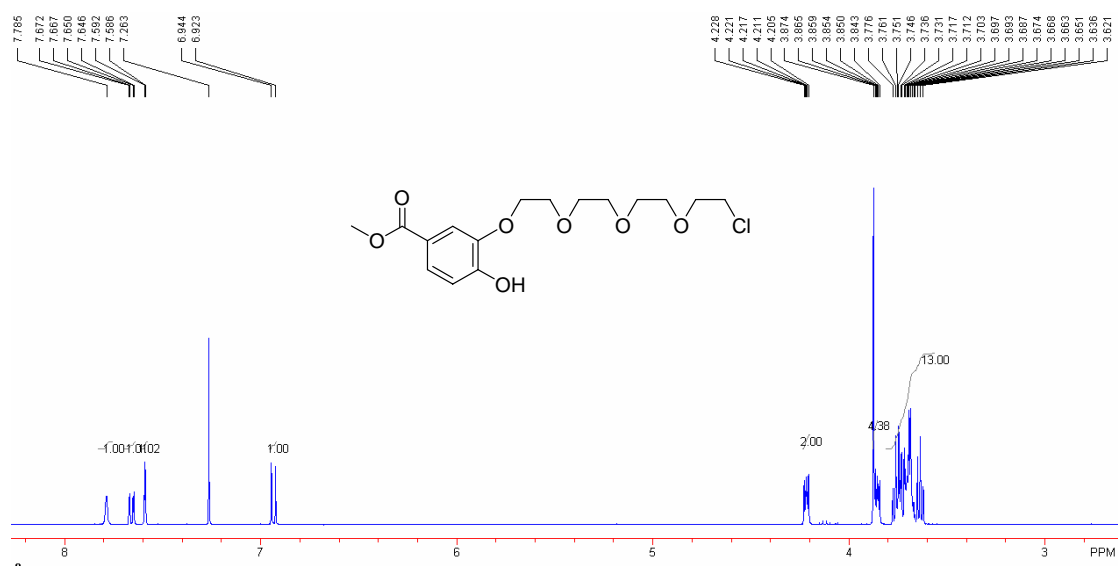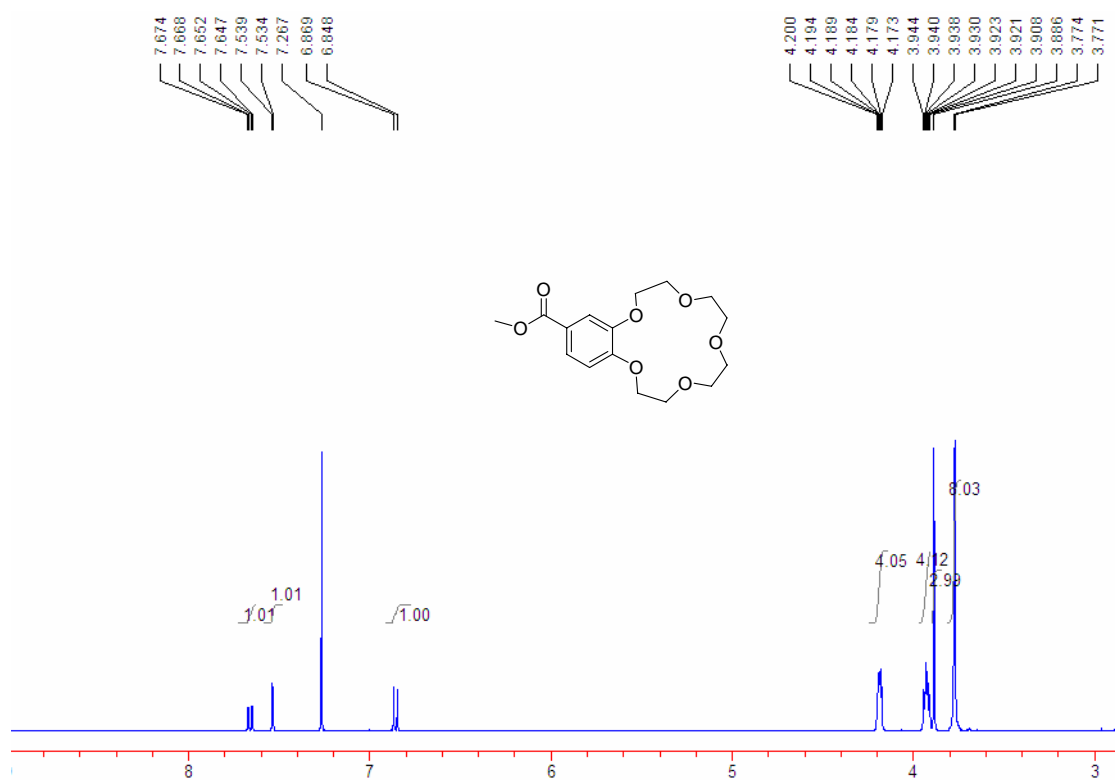**FIGURE S8.** ^{1}H NMR spectrum (400 MHz, CDCl$_3$, 22 °C) of **8**.

FIGURE S9. ^{1}H NMR spectrum (400 MHz, CD$_3$COCD$_3$, 22 °C) of **9**.

FIGURE S10. ^{1}H NMR spectrum (400 MHz, CD$_3$COCD$_3$, 22 °C) of **10**.

FIGURE S11. ^{1}H NMR spectrum (400 MHz, CD$_3$COCD$_3$, 22 °C) of **1**.

FIGURE S12. ^{1}H NMR spectrum (400 MHz, CD$_3$COCD$_3$, 22 °C) of **11**.

FIGURE S13. ^{1}H NMR spectrum (400 MHz, CDCl$_3$, 22 °C) of **12**.
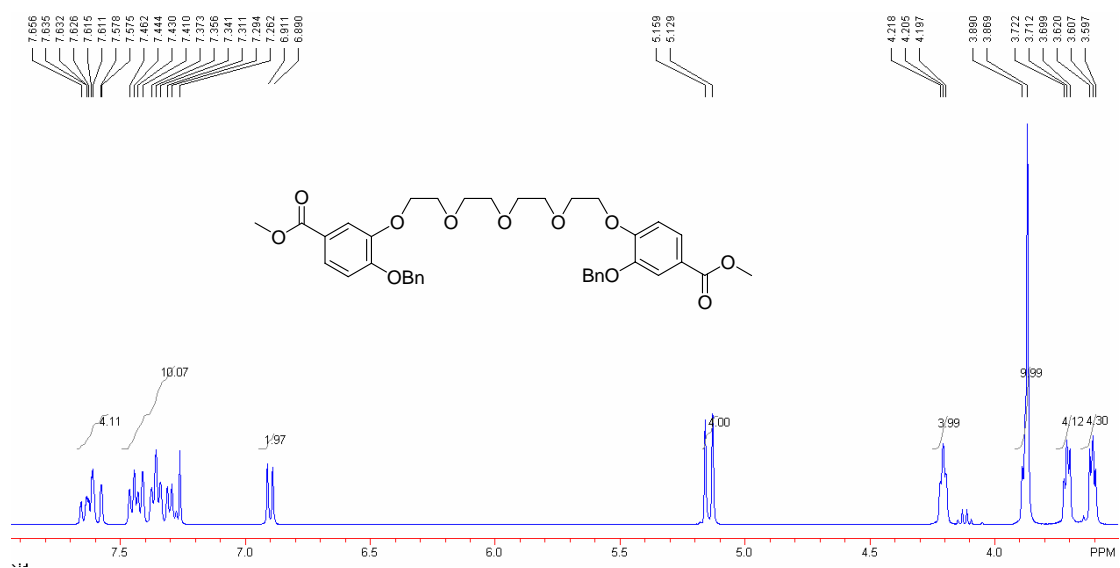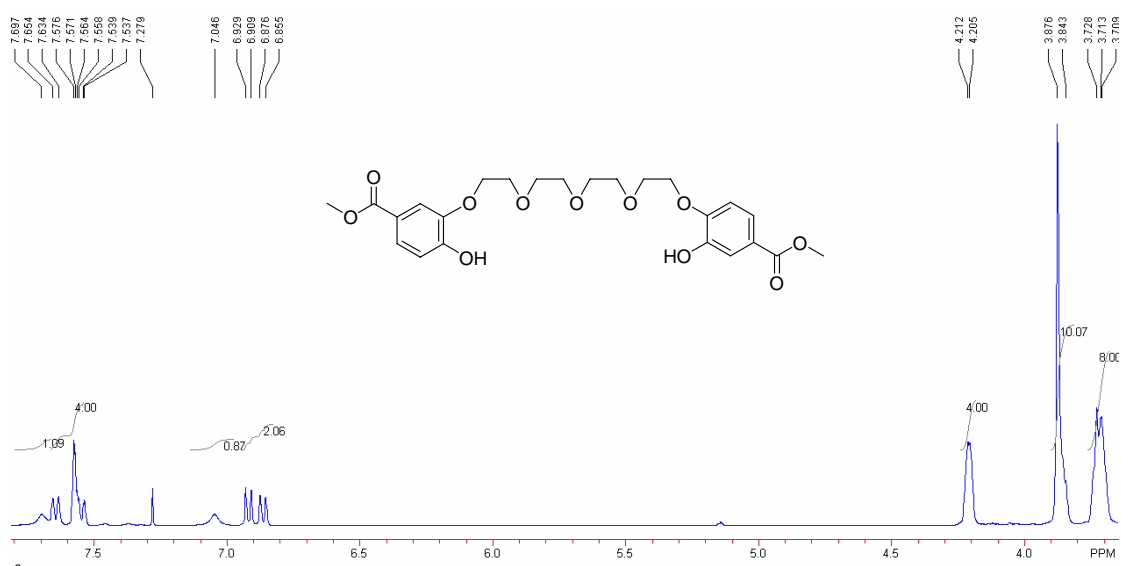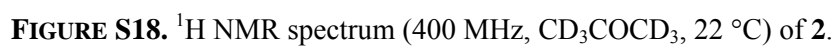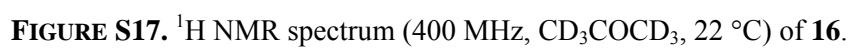

**FIGURE S14.** ^{1}H NMR spectrum (400 MHz, CDCl$_3$, 22 °C) of **13**.

FIGURE S15. ^{1}H NMR spectrum (400 MHz, CDCl$_3$, 22 °C) of **14**.

FIGURE S16. ^{1}H NMR spectrum (400 MHz, CD$_3$COCD$_3$, 22 °C) of **15**.

**FIGURE S17.** ^{1}H NMR spectrum (400 MHz, CD$_3$COCD$_3$, 22 °C) of **16**.

**FIGURE S18.** ^{1}H NMR spectrum (400 MHz, CD$_3$COCD$_3$, 22 °C) of **2**.

3. Electrospray ionization mass spectra of equimolar acetone solutions of either of hosts 1 and 2 with either of guests 3 and 4
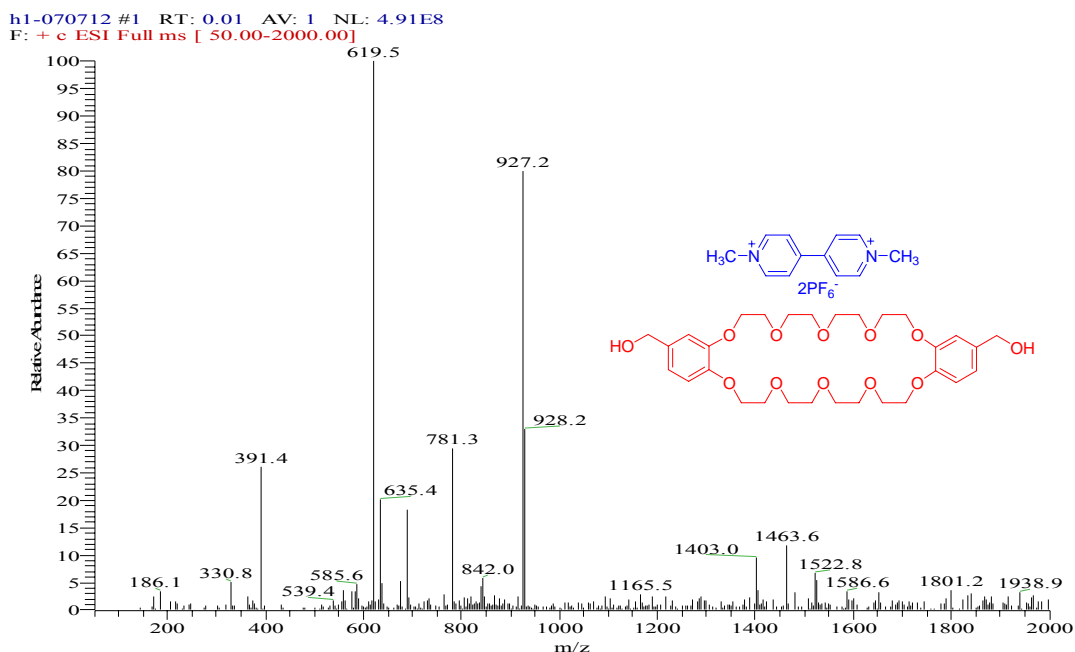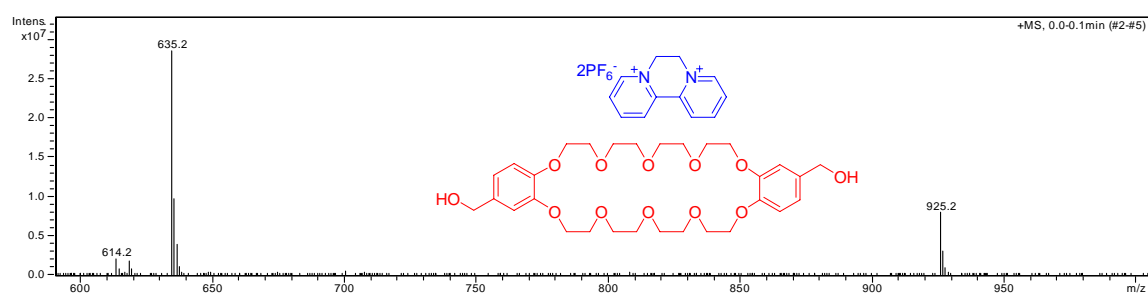

FIGURE S19. Electrospray ionization of mass spectrum of an equimolar solution of **1** with **3**. Assignment of main peaks: m/z 927.2 $[\mathbf{1} \bullet \mathbf{3} - PF_6]^+$ (79%), 781.3 $[\mathbf{1} \bullet \mathbf{3} - PF_6 - HPF_6]^+$ (29%), 635.4 $[\mathbf{1} + K]^+$ (20%), 619.5 $[\mathbf{1} + Na]^+$ (100%), and 391.4 $[\mathbf{1} \bullet \mathbf{3} - 2PF_6]^{2+}$ (25%).
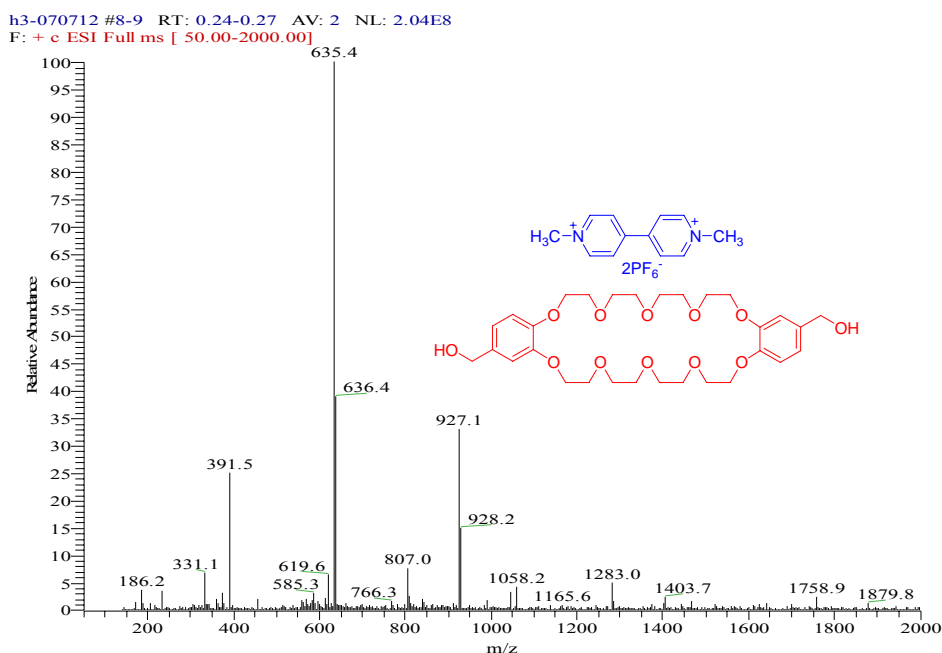
FIGURE S20. Electrospray ionization of mass spectrum of an equimolar solution of **2** with **3**. m/z 927.2 $[\mathbf{2} \bullet \mathbf{3} - PF_6]^+$ (32%), 635.4 $[\mathbf{2} + K]^+$ (100%), and 391.5 $[\mathbf{2} \bullet \mathbf{3} - 2PF_6]^{2+}$ (25%).
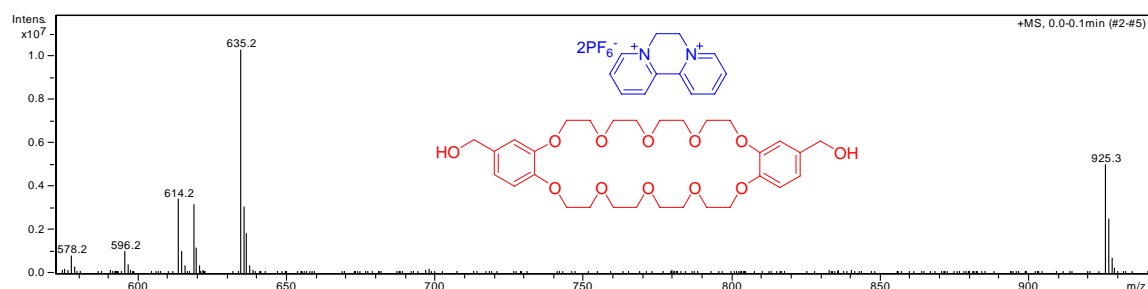
FIGURE S21. Electrospray ionization of mass spectrum of an equimolar solution of **1** with **4**.

m/z 925.2 [**1•4** − PF$_6$]$^+$ (42%), 635.2 [**1** + K]$^+$ (100%), 619.3 [**1** + Na]$^+$ (34%), 614.2 [**1** + H$_2$O]$^+$ (36%), 596.2 [**1**]$^+$ (11%), and 578.2 [**1** − H$_2$O]$^+$ (8%).

FIGURE S22. Electrospray ionization of mass spectrum of an equimolar solution of **2** with **4**.

*m/z* 925.2 [**2•4** − PF$_6$]$^+$ (18%), 635.2 [**2** + K]$^+$ (100%), and 614.2 [**2** + H$_2$O]$^+$ (7%).

4. X-ray analysis data of *1•4* and *2•4*

X-ray analysis data of 1•4: Crystallographic data: plate, red, $0.35 \times 0.24 \times 0.15$ mm^3, $C_{42}H_{58}F_{12}N_2O_{15}P_2$, *FW* 1120.84, orthorhombic, space group Cmc2$_1$, $a = 20.757(7)$, $b = 10.663(2)$, $c = 22.319(5)$ Å, $\alpha = \beta = \gamma = 90.00°$, $V = 4940(2)$ Å^3, $Z = 4$, $D_c = 1.507$ g cm^{-3}, $T = 100(2)$ K, $\mu = 0.201$ mm^{-1}, 19011 measured reflections, 4268 independent reflections, 367 parameters, 227 restraints, $F(000) = 2328$, $R_1 = 0.2549$, $wR_2 = 0.3829$ (all data), $R_1 = 0.1309$, $wR_2 = 0.3018$ [$I > 2\sigma(I)$], max. residual density 0.555 e•Å^{-3}, and goodness-of-fit (F^2) = 1.068. The high R_1 and wR_2 values and poor mean C-C bond length precision are mainly due to the severe disorder of the crystal structure. We tried our best, including growing crystals in different solvent systems and doing data collections on different single crystals at low temperature, but no better data set could be obtained. Although the present data set is not good, the framework can be clearly solved and the crystallographic data strongly supports the spectroscopic characterizations.

X-ray analysis data of 2•4: Crystallographic data: prism, red, $0.503 \times 0.482 \times 0.371$ mm^3, $C_{42}H_{56}F_{12}N_2O_{12}P_2$, *FW* 1070.83, orthorhombic, space group P2$_1$2$_1$2$_1$, $a = 11.3885(13)$, $b = 18.885(2)$, $c = 22.602(3)$ Å, $\alpha = \beta = \gamma = 90.00°$, $V = 4861.0(10)$ Å^3, $Z = 4$, $D_c = 1.463$ g cm^{-3}, $T = 100(2)$ K, $\mu = 0.196$ mm^{-1}, 26463 measured reflections, 9457 independent reflections, 636 parameters, 3 restraints, $F(000) = 2224$, $R_1 = 0.1361$, $wR_2 = 0.2000$ (all data), $R_1 = 0.0715$, $wR_2 = 0.1757$ [$I > 2\sigma(I)$], max. residual density 0.551 e•Å^{-3}, and goodness-of-fit (F^2) = 0.878.
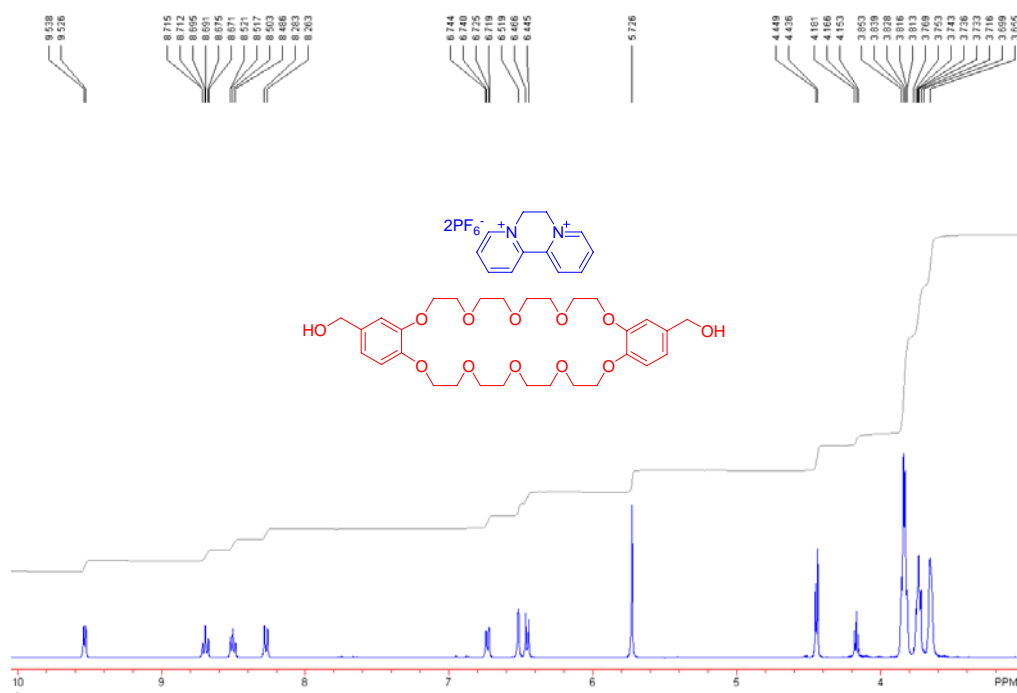
*5. Partial ^1H NMR spectra of equimolar solutions of either of hosts **1** and*
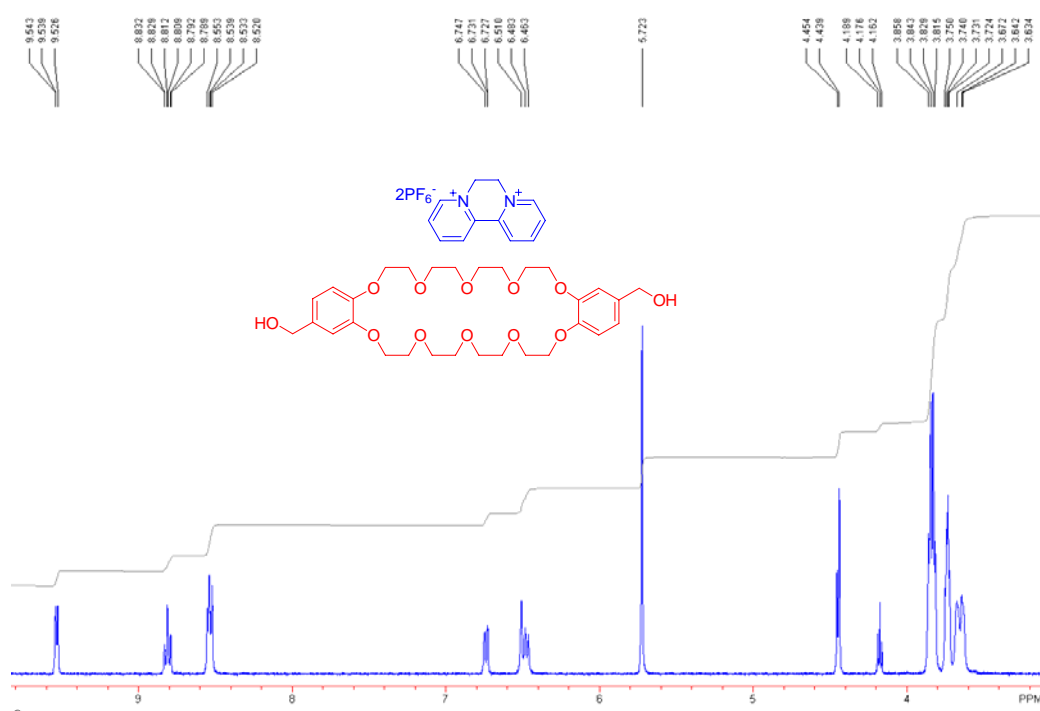
***2** with either of guests **3** and **4** in CD₃COCD₃*
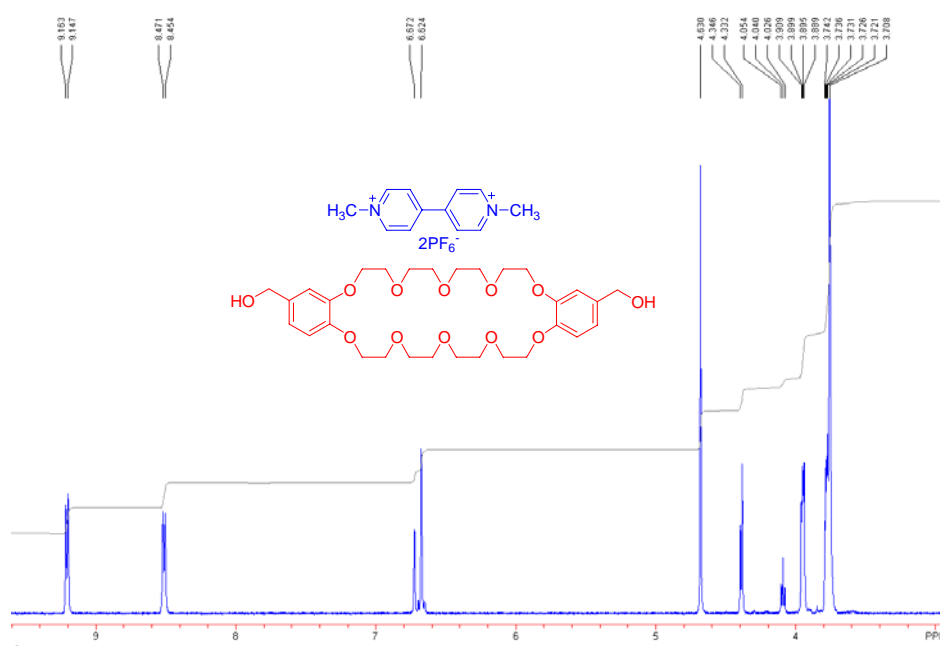
FIGURE S23. Partial ^1H NMR spectrum (400 MHz, CD₃COCD₃, 22 °C) of an equimolar (4.00 mM) solution of **1** with **3**.
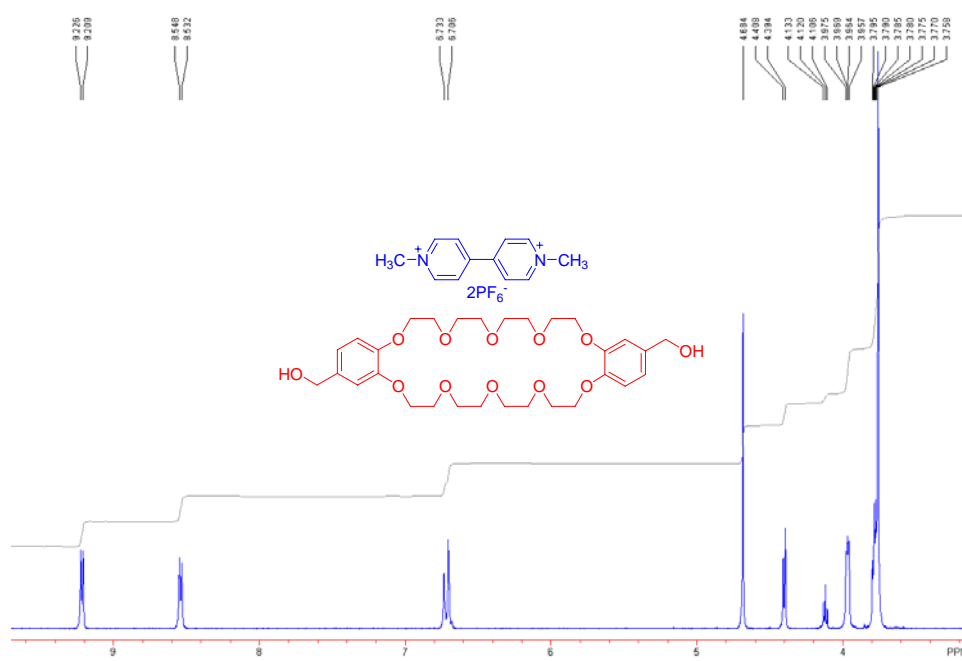
FIGURE S24. Partial ^1H NMR spectrum (400 MHz, CD₃COCD₃, 22 °C) an equimolar (4.00 mM) solution of **2** with **3**.

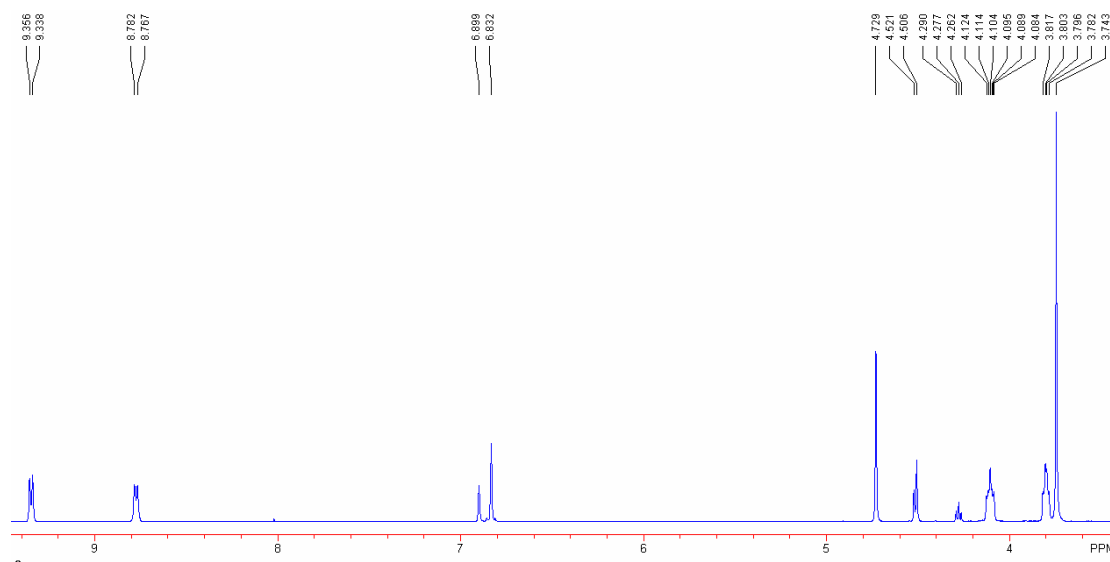**FIGURE S25.** Partial ^{1}H NMR spectrum (400 MHz, CD$_3$COCD$_3$, 22 °C) an equimolar (4.00 mM) solution of **1** with **4**.

FIGURE S26. Partial ^{1}H NMR spectrum (400 MHz, CD$_3$COCD$_3$, 22 °C) of an equimolar (4.00 mM) solution of **2** with **4**.
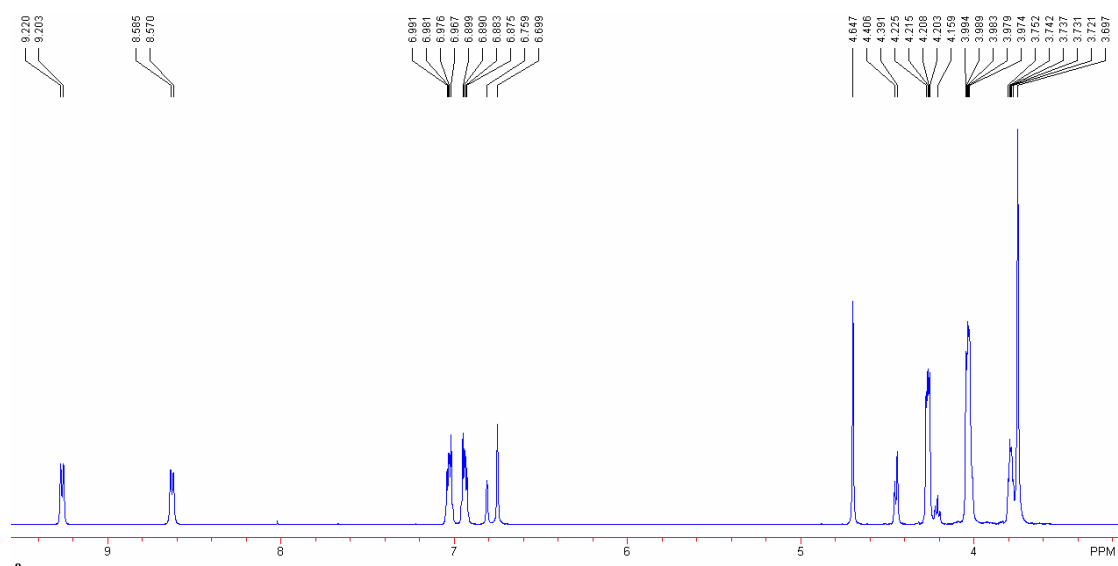
*6. Partial ^1H NMR spectra demonstrating control of complexations between either of hosts **1** and **2** with either of guests **3** and **4** by additions of small molecules KPF_6 and dibenzo-18-crown-6 in CD_3COCD_3*

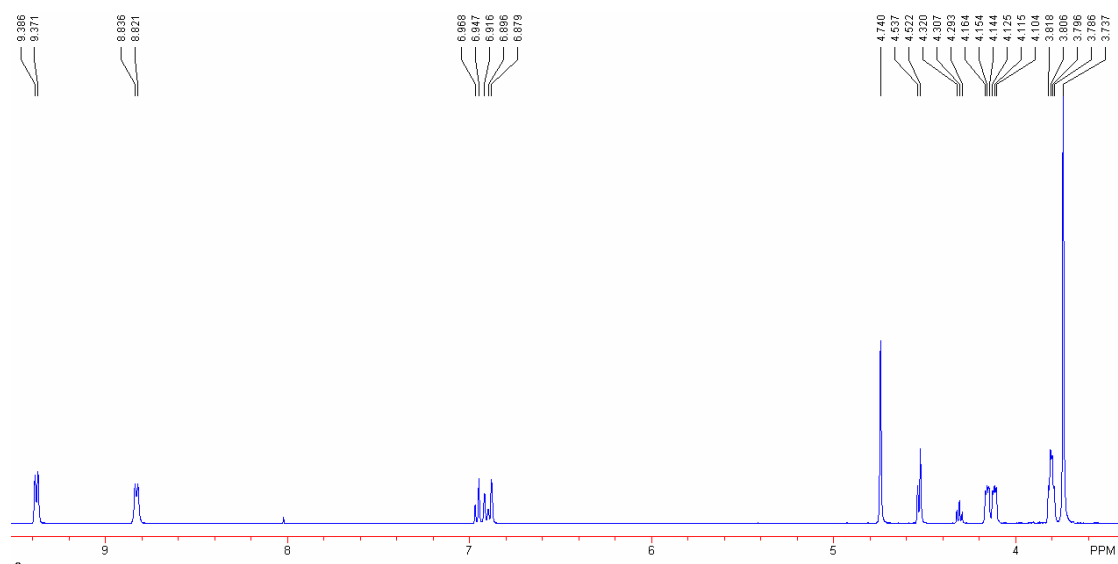**FIGURE S27.** Partial ^{1}H NMR spectrum (400 MHz, CD_3COCD_3, 22 °C) of 4.00 mM **1**, **3** and KPF_6.
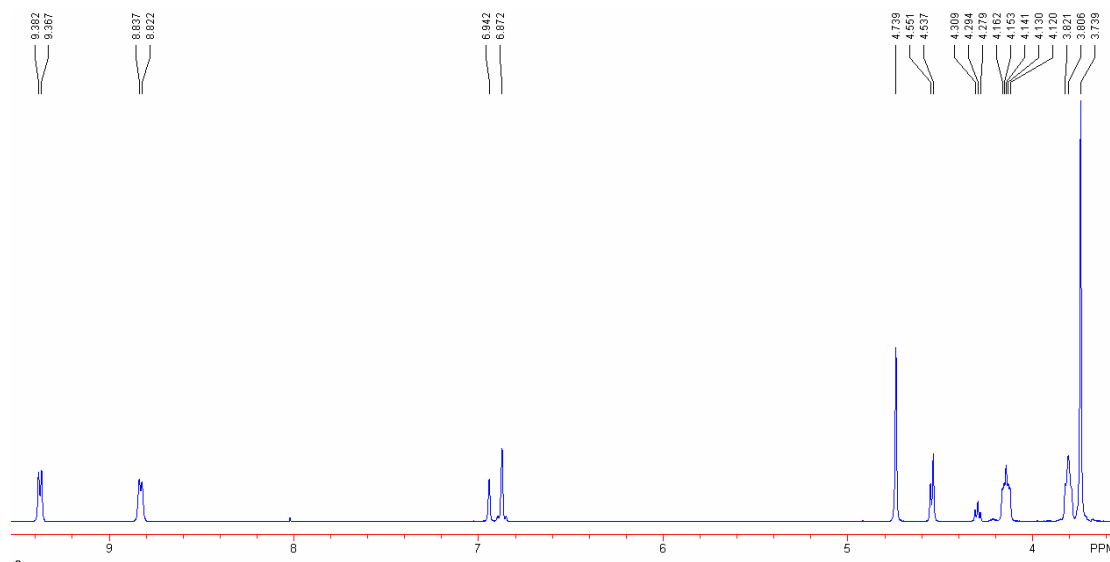
FIGURE S28. Partial ^{1}H NMR spectrum (400 MHz, CD_3COCD_3, 22 °C) of 4.00 mM **1** and **3** and 8.00 mM KPF_6.

FIGURE S29. Partial ^{1}H NMR spectrum (400 MHz, CD$_3$COCD$_3$, 22 °C) of 4.00 mM **1** and **3** and 8.00 mM KPF$_6$ and DB18C6.

FIGURE S30. Partial ^{1}H NMR spectrum (400 MHz, CD$_3$COCD$_3$, 22 °C) of 4.00 mM **2**, **3** and KPF$_6$.
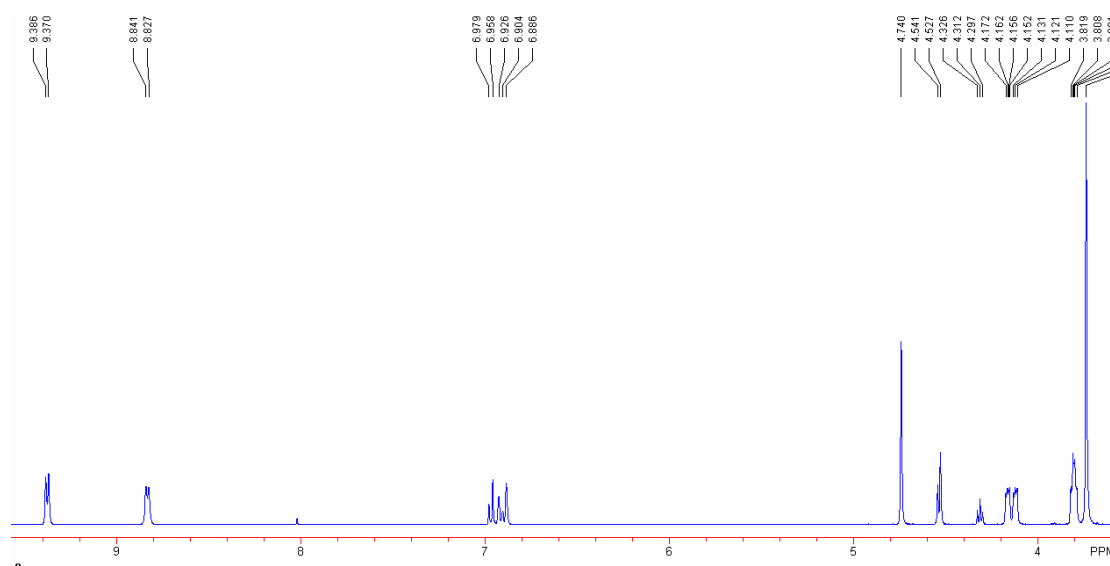
FIGURE S31. Partial ^{1}H NMR spectrum (400 MHz, CD$_3$COCD$_3$, 22 °C) of 4.00 mM **2** and **3** and 8.00 mM KPF$_6$.
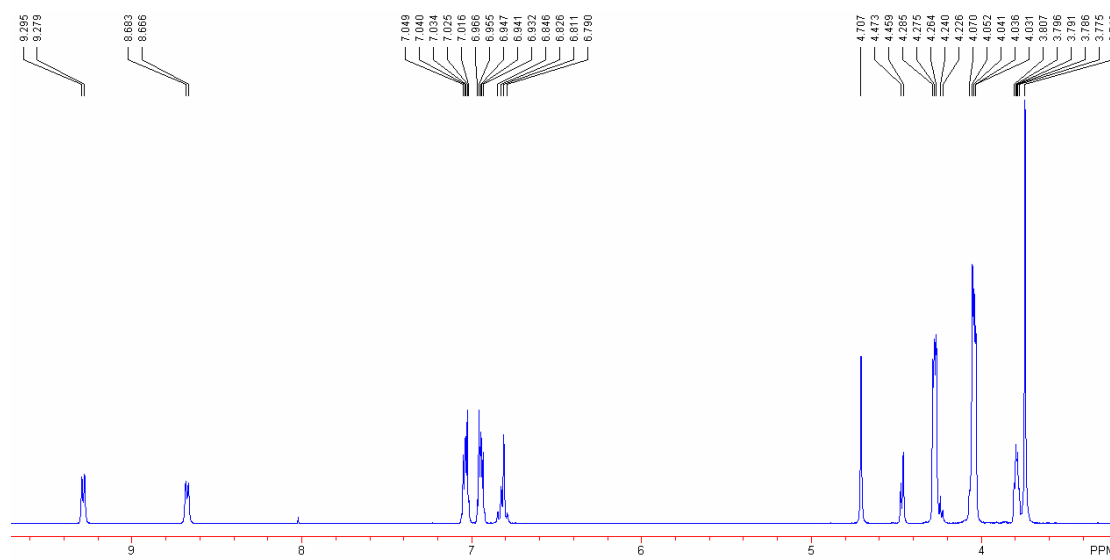
FIGURE S32. Partial ^{1}H NMR spectrum (400 MHz, CD$_3$COCD$_3$, 22 °C) of 4.00 mM **2** and **3** and 8.00 mM KPF$_6$ and DB18C6.
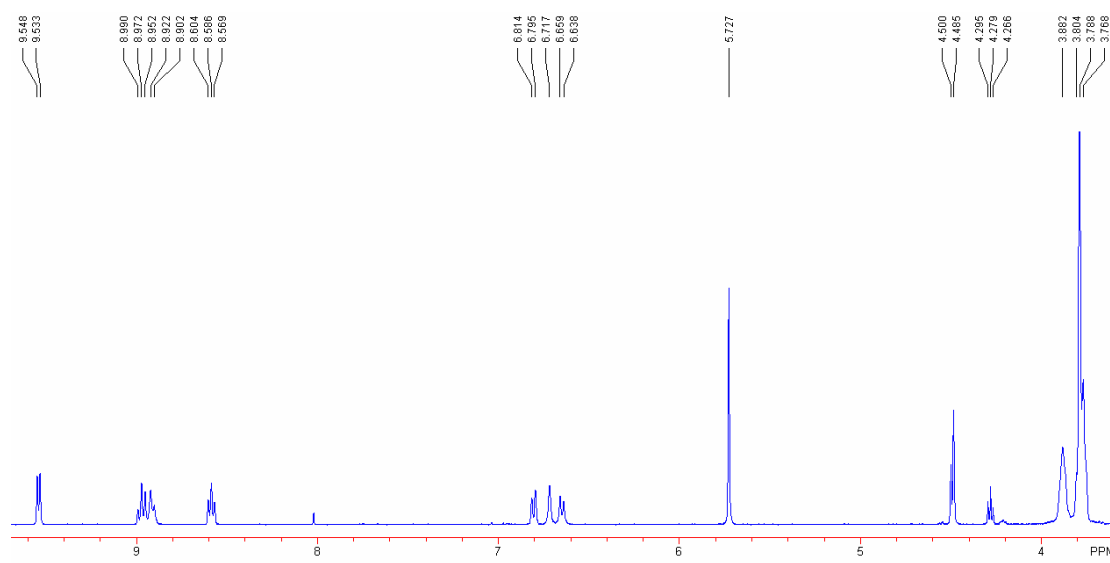
FIGURE S33. Partial ^{1}H NMR spectrum (400 MHz, CD$_3$COCD$_3$, 22 °C) of 4.00 mM **1**, **4** and KPF$_6$.
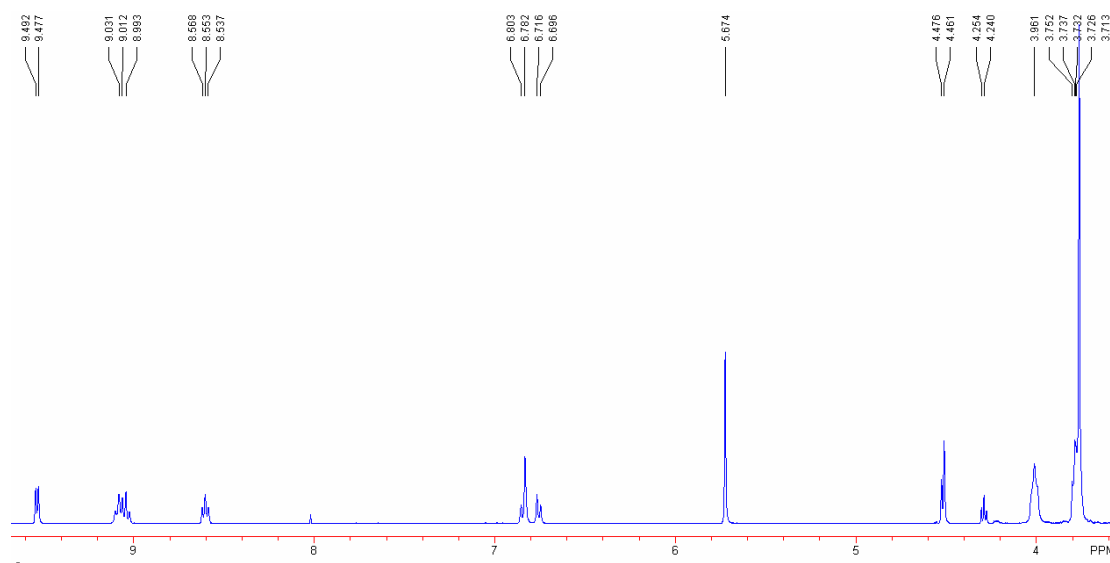
FIGURE S34. Partial ^{1}H NMR spectrum (400 MHz, CD$_3$COCD$_3$, 22 °C) of 4.00 mM **1** and **4** and 8.00 mM KPF$_6$.
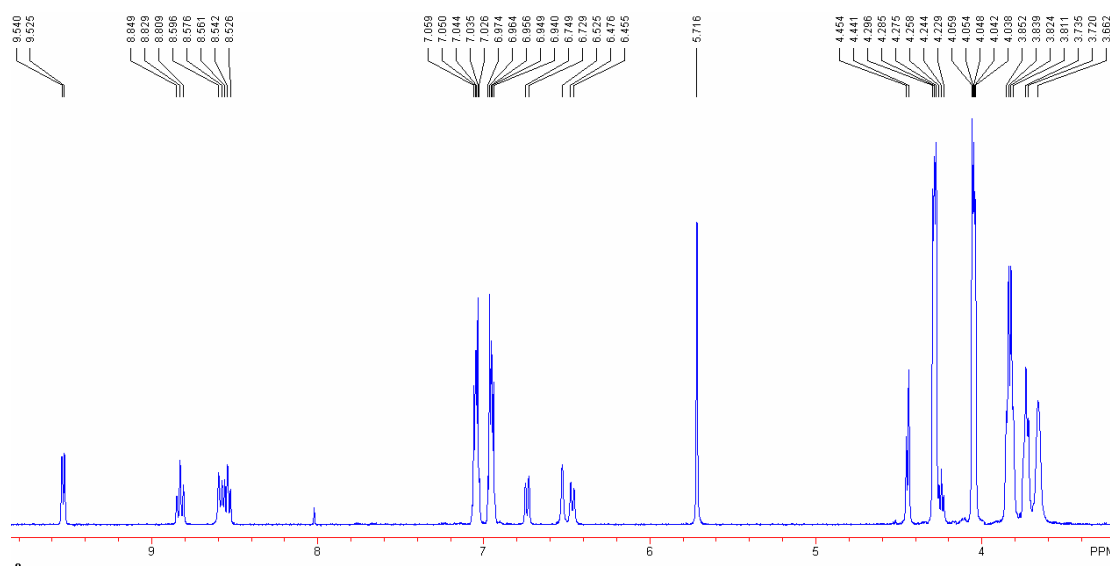
FIGURE S35. Partial ^{1}H NMR spectrum (400 MHz, CD$_3$COCD$_3$, 22 °C) of 4.00 mM **1** and **4** and 8.00 mM KPF$_6$ and DB18C6.
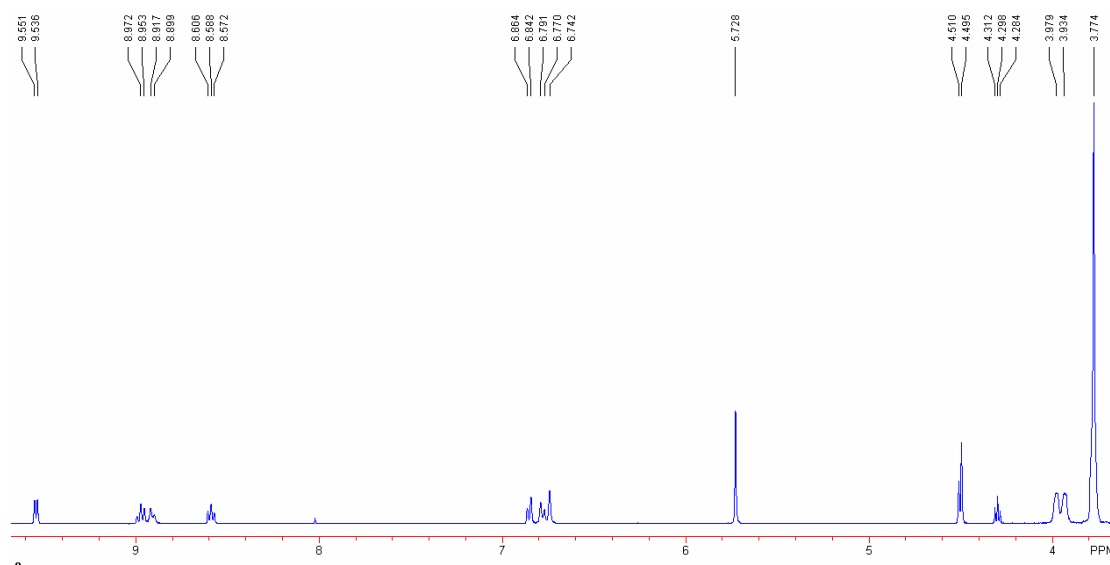
FIGURE S36. Partial ^{1}H NMR spectrum (400 MHz, CD$_3$COCD$_3$, 22 °C) of 4.00 mM **2**, **4** and KPF$_6$.
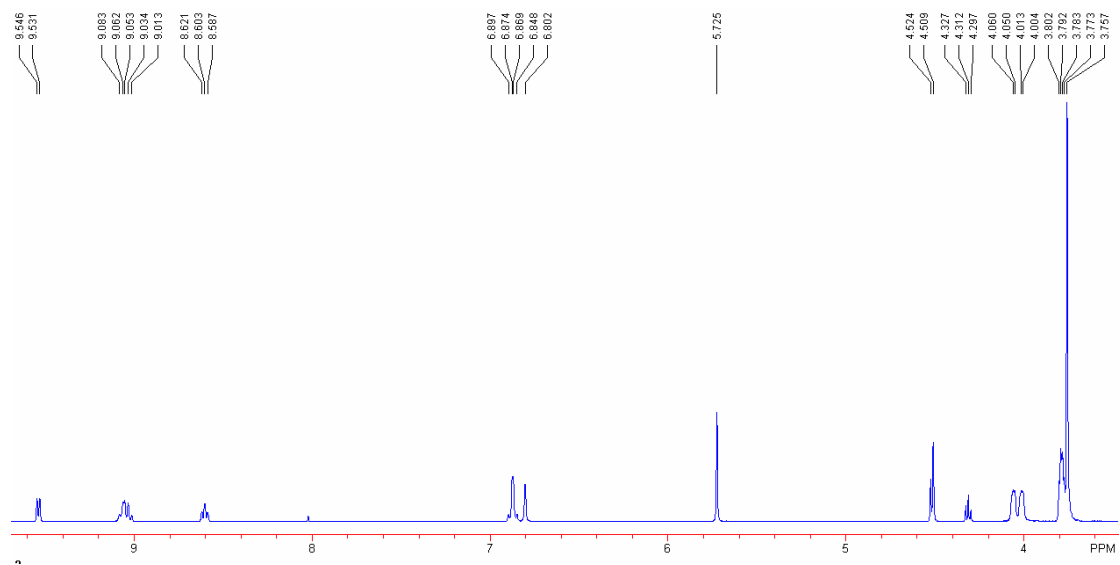
FIGURE S37. Partial ^{1}H NMR spectrum (400 MHz, CD$_3$COCD$_3$, 22 °C) of 4.00 mM **2** and **4** and 8.00 mM KPF$_6$.
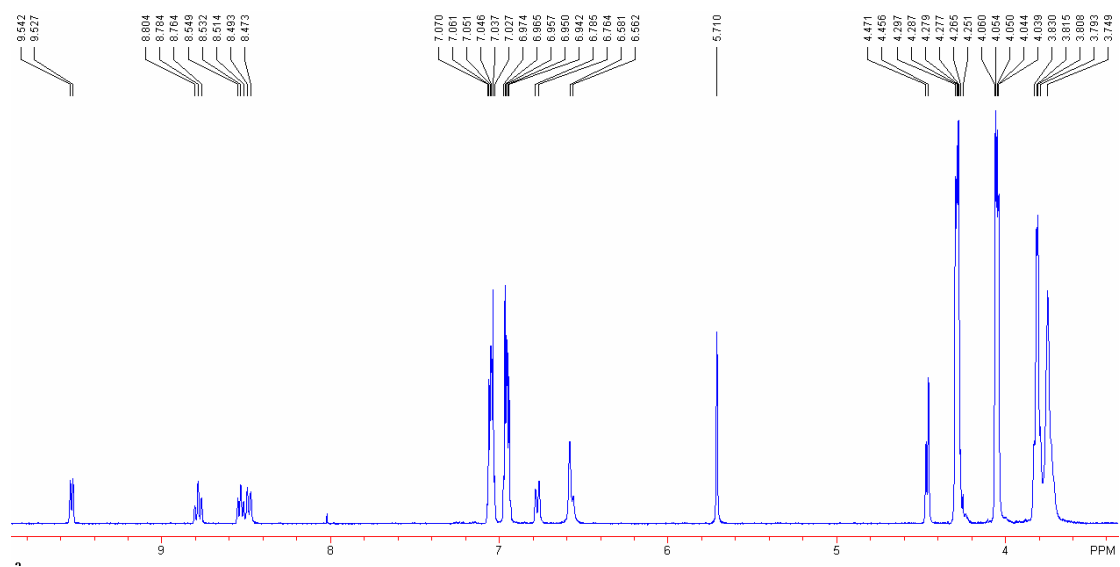
FIGURE S38. Partial ^{1}H NMR spectrum (400 MHz, CD$_3$COCD$_3$, 22 °C) of 4.00 mM **2** and **4** and 8.00 mM KPF$_6$ and DB18C6.

7. General experimental methods and preparations of known compounds

Tetrahydrogenfuran (THF) was distilled in the presence of sodium. Dimethylformamide (DMF) was dried by distillation in the presence of CaH_2. Other chemicals were reagent grade and used as received. Compounds **3**[S2b] and **4**[S2a] were prepared according to the literature, respectively.

Methyl 3,4-Dihydroxybenzoate (6).[S3] To a stirred solution of 3,4-dihydroxybenzoic acid (15.4 g, 100 mmol) in CH_3OH (150 mL) was added $SOCl_2$ (15.0 mL, 126 mmol) dropwise over 1 hour at 0 °C. The mixture solution was further stirred at reflux for 12 hours. After solvent removal, the solid was dissolved in CH_2Cl_2 and washed twice with saturated Na_2CO_3 solution and dried over anhydrous Na_2SO_4. After CH_2Cl_2 was evaporated, the residue was recrystallized in water to yield **6** as a white solid (15.1 g, 90%). Mp. 140–142 °C (lit. 141.8–142.7 °C[17]); ^1H NMR (400 MHz, CD_3COCD_3, 22 °C): δ 8.63 (s, 1H), 8.31 (s, 1H), 7.50 (d, J = 2.4 Hz, 1H), 7.44 (dd, J_1 = 8.4 Hz, J_2 = 2.4 Hz, 1H), 6.90 (d, J = 8.4 Hz, 1H), 3.80 (s, 3H).

Methyl 4-benzyloxy-3-hydroxybenzoate (7a) and Methyl 3-benzyloxy-4-hydroxybenzoate (7b).[S3] To a stirred suspension of methyl 3,4-dihydroxybenzoate **6** (8.40 g, 50.0 mmol) and K_2CO_3 (6.90 g, 50.0 mmol) in CH_3CN (150 mL) was added benzyl bromide (8.55 g, 50.0 mmol) dropwise over a period of 5 hours under N_2 atmosphere at room temperature. The resulted suspension was stirred at reflux for another 24 hours. The mixture was filtered. After solvent removal, the residue was dissolved in CH_2Cl_2 and washed twice with saturated Na_2CO_3 solution. CH_2Cl_2 was removed. The crude product was absorbed on silica gel and purified by flash column chromatography (ethyl acetate/petroleum ether = 8/50) to give **7a** as a white solid (6.45 g, 50%) and **7b** as a white solid (2.58 g, 20%). **7a** Mp. 132–133 °C (lit. 133.7–135.0 °C[17]); ^1H NMR (400 MHz, $CDCl_3$, 22 °C): δ 7.63–7.59 (m, 2H), 7.43–739 (m, 5H), 6.95 (d, J = 4.0 Hz, 1H), 5.72 (s, 1H), 5.18 (s, 2H), 3.89 (s, 3H). **7b** Mp. 127–129 °C; ^1H NMR (400 MHz, $CDCl_3$, 22 °C): δ 7.67–7.65 (m, 2H), 7.45–7.38 (m, 5H), 6.96 (d, J = 4.0 Hz, 1H), 5.17 (s, 2H), 3.89 (s, 3H). Anal.

Calcd for $C_{15}H_{14}O_4$: C, 69.76; H, 5.46. Found: C, 69.80; H, 5.44.

Carbomethoxybenzo-15-crown-5 (13).[S4] A suspension of **12** (0.720 g, 2.00 mmol) and K_2CO_3 (1.40 g, 10.0 mmol) in CH_3CN (80.0 mL) was stirred under N_2 atmosphere at reflux for 24 h. After filtration, the solvent of the filtrate was removed under reduced pressure. The residue was dissolved in CH_2Cl_2 and washed twice with water. The solvent was removed to afford a crude product, which was was absorbed on silica gel and purified by column chromatography to give **13** as a white solid (0.59 g, 90%). Mp. 74–76 °C; ^{1}H NMR (400 MHz, CDCl₃, 22 °C): δ 7.66 (dd, $J_1 = 8.4$ Hz, $J_2 = 2.0$ Hz, 1H), 7.53 (d, $J = 2.0$ Hz, 1H), 6.85 (d, $J = 8.4$ Hz, 1H), 4.20–4.17 (m, 4H), 3.94–3.91 (m, 4H), 3.88 (s, 3H), 3.77 (s, 8H).
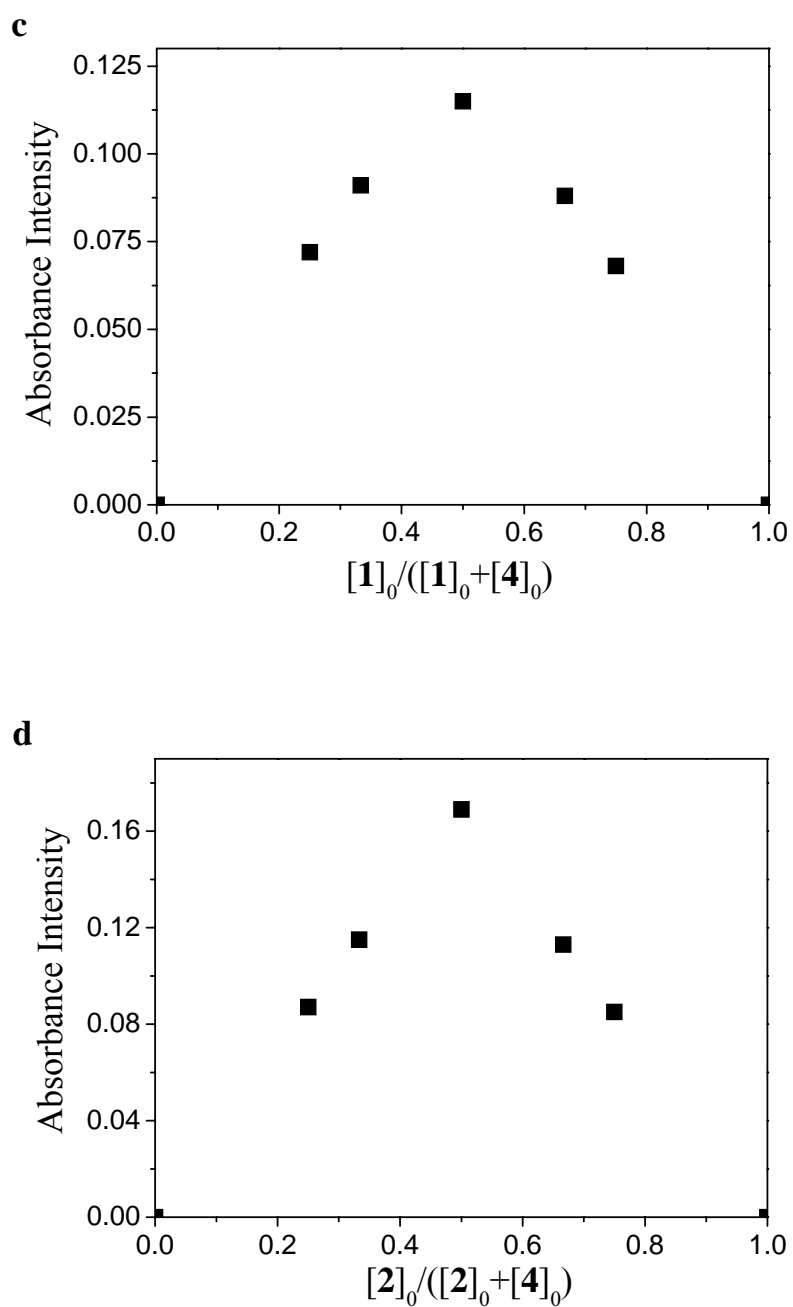
*8. Job plots of **1•3**, **2•3**, **1•4**, and **2•4** based on UV-Vis data in acetone*

a

b

c

d
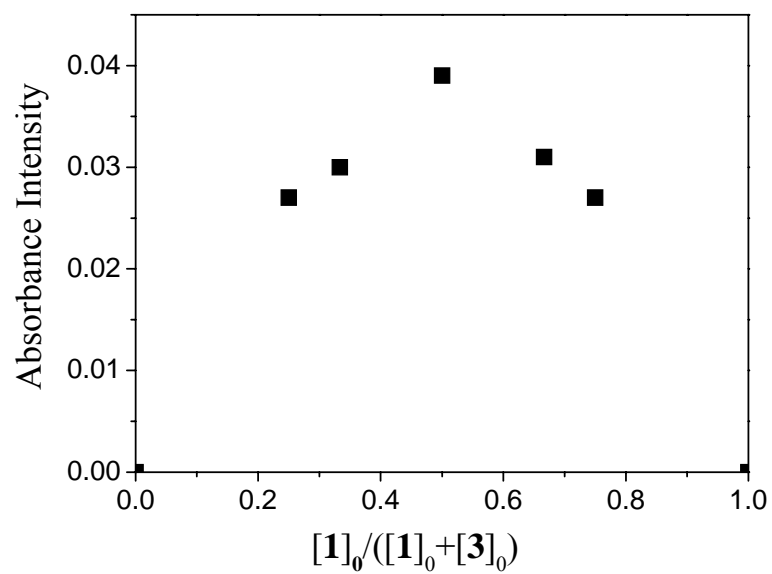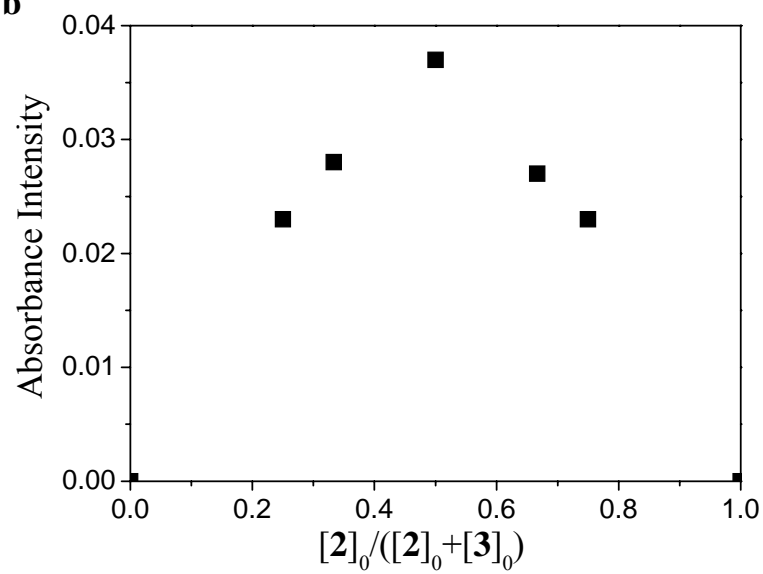
**FIGURE S39.** Job plots showing the 1:1 stoichiometries of the complexes between **1** and **3** (a), **2** and **3** (b), **1** and **4** (c), and **2** and **4** (d) in acetone: (a) $[1]_0 + [3]_0 = 1.00$ mM; (b) $[2]_0 + [3]_0 = 1.00$ mM; (c) $[1]_0 + [4]_0 = 1.00$ mM; (d) $[2]_0 + [4]_0 = 1.00$ mM. $[1]_0$, $[2]_0$, $[3]_0$, $[4]_0$ are the initial concentration of **1**, **2**, **3** and **4,** respectively.

*9. The ^1H NMR spectra related to the studies on the complexations of **2** with either of **3** and **4** and the effects of the additions of small molecules KPF$_6$ and dibenzo-18-crown-6 on them*
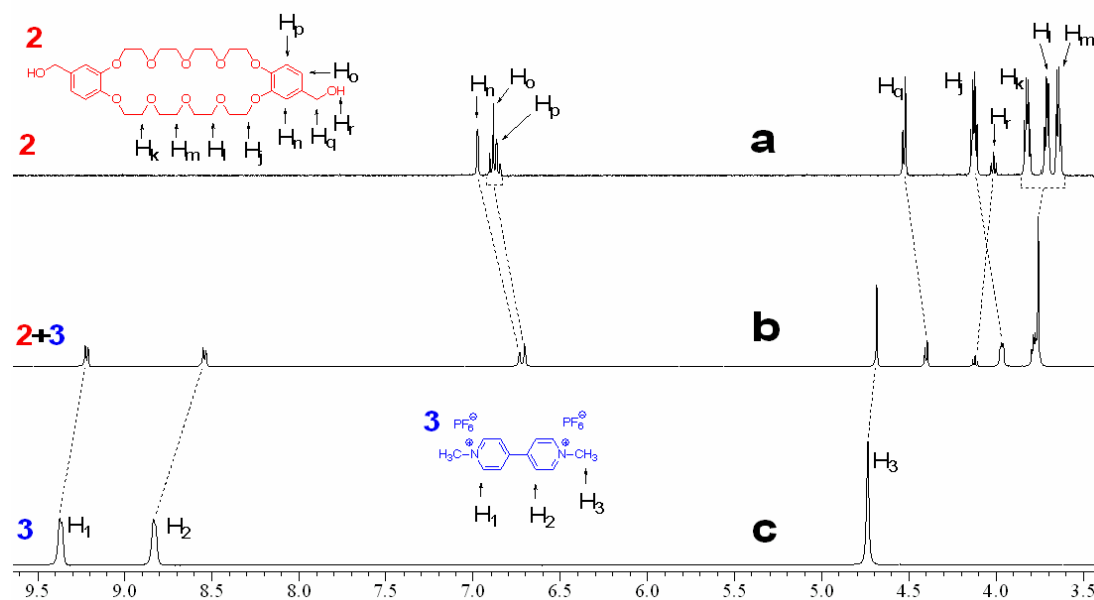
FIGURE S40. Partial ^{1}H NMR spectra (400 MHz, 22 °C) of 4.00 mM crown ether **2** (a), 4.00 mM crown ether **2** and paraquat **3** (b), and 4.00 mM paraquat **3** (c) in acetone-d_6.
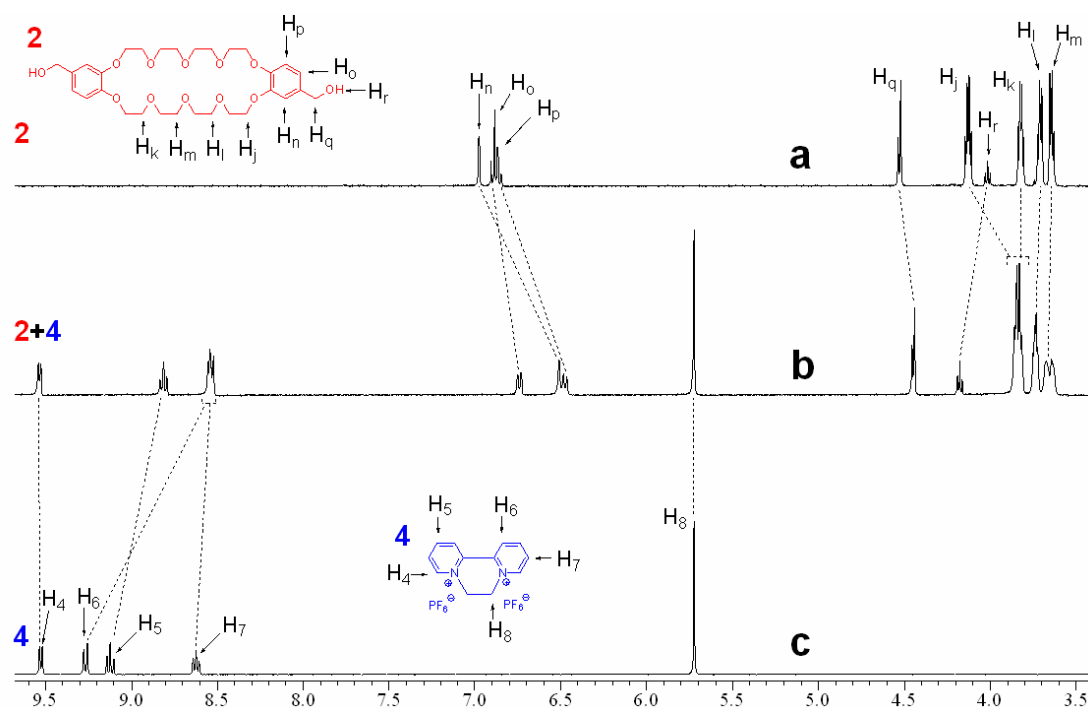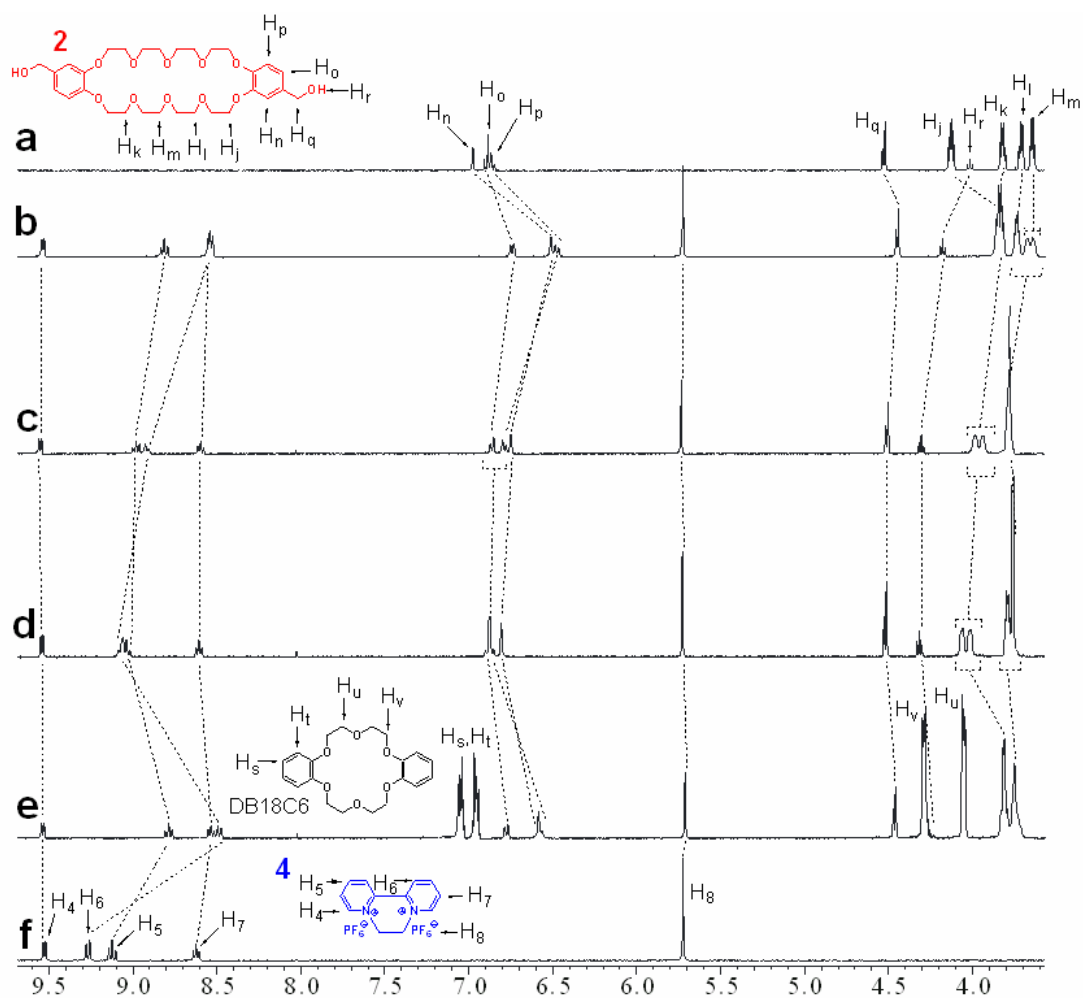
FIGURE 41. Partial ^{1}H NMR spectra (400 MHz, 22 °C) of 4.00 mM crown ether **2** (a), 4.00 mM crown ether **2** and diquat **4** (b), and 4.00 mM diquat **4** (c) in acetone-d_6.
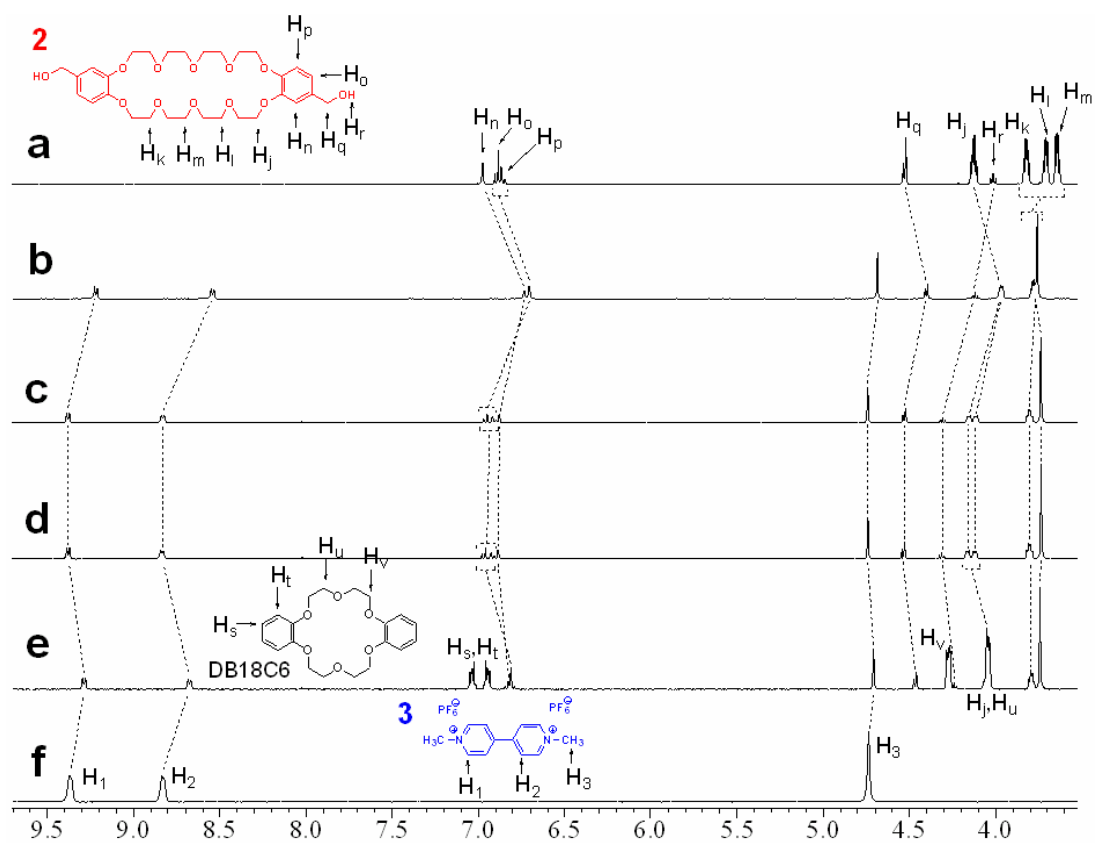
FIGURE 42. Partial 400 MHz ^{1}H NMR spectra of (a) 4.00 mM **2**, (b) 4.00 mM **2** and **3**, (c) 4.00 mM **2**, **3** and KPF$_6$, (d) 4.00 mM **2** and **3** and 8.00 mM KPF$_6$, (e) 4.00 mM **2** and **3** and 8.00 mM KPF$_6$ and DB18C6, and (f) 4.00 mM **3** in acetone-d_6.

FIGURE 43. Partial 400 MHz ^{1}H NMR spectra of (a) 4.00 mM **2**, (b) 4.00 mM **2** and **4**, (c) 4.00 mM **2**, **4** and KPF$_6$, (d) 4.00 mM **2** and **4** and 8.00 mM KPF$_6$, (e) 4.00 mM **2** and **4** and 8.00 mM KPF$_6$ and DB18C6, and (f) 4.00 mM **4** in acetone-d_6.

References

S1. Connors, K. A. Binding Constants; Wiley: New York, 1987. Corbin, P. S. Ph.D. Dissertation, University of Illinois at Urbana-Champaign, Urbana, IL, 1999. Ashton, P. R.; Ballardini, R.; Balzani, V.; Belohradsky, M.; Gandolfi, M. T.; Philp, D.; Prodi, L.; Raymo, F. M.; Reddington, M. V.; Spencer, N.; Stoddart, J. F.; Venturi, M.; and Williams, D. J. *J. Am. Chem. Soc.* **1996**, *118*, 4931-4951.

S2. (a) Summers, L. A. *Tetrahedron* **1968**, *24*, 2697–2700. (b) Luong, J. C.; Nadjo, L.; Wrighton, M. S. *J. Am. Chem. Soc.* **1978**, *100*, 5790–5795.

S3. Gibson, H. W.; Wang, H.; Bonrad, K.; Jones, J. W.; Slebodnick, C.; Zackharov, L. N.; Rheingold, A. L.; Habenicht, B.; Lobue, P.; Ratliff, A. E. *Org. Biomol. Chem.* **2005**, *3*, 2114–2121.

S4. Shinkai, S.; Nishi, T.o; Ikeda, A.; Matsuda, T.; Shimamoto, K.; Manabe, O. *J. Chem. Soc., Chem. Comm.* **1990**, 303–304.